Automated spectral and timing analysis of AGNs

Filip Munz[1], **Vladimir Karas**[1], and **Matteo Guainazzi**[2]

[1] Astronomical Institute, Academy of Sciences of Czech Republic
[2] European Space Astronomy Center, Madrid, Spain

Received 13 Sep 2006
Published online later

Key words x-rays;time resolved spectra

We have developed an autonomous script that helps the user to automate the XMM-Newton data analysis for the purposes of extensive statistical investigations. We test this approach by examining X-ray spectra of bright AGNs pre-selected from the public database. The event-lists extracted in this process were studied further by constructing their energy-resolved Fourier power-spectrum density. This analysis combines energy distributions, light-curves, and their power-spectra and it proves useful to assess the variability patterns present is the data. As another example, an automated search was based on the XSPEC package to reveal the emission features in 2-8 keV range.

1 Introduction

The emission complex of iron, in particular the Kα line, is the most prominent feature in X-ray spectra of a large number of active galactic nuclei (AGN) within the 2–8 keV energy band. In several cases the observed spectra are compatible with a skewed two-horn profile, expected on theoretical grounds for the disk–line geometry; these spectra exhibit the relativistic broadening and the Doppler/gravitational energy shifts which arise as a result of the interplay among fast motion of the emitting gas, strong-gravity effects, and the effect of integration of the reflection component over the surface of an accretion disk.

If time bins of the observation are sufficiently short, so that the reflection can be localized in time (requiring a sufficiently sensitive device), the emission line is expected to be narrow – similar to the intrinsic profile. The narrow line can be shifted in energy with respect to the intrinsic (rest-frame) emission. The existence of these narrow iron lines was reported in spectra of NGC 3516 (Turner et al 2002), NGC 7314 (Yaqoob et al 2003), ESO 198-G024 (Dovčiak et al 2004), and Mkn 776 (Turner et al 2006). Searching for such features is one of potential uses of our computational tool. In this paper we describe our technique and preliminary results in which the script was applied to perform an automated analysis of a large dataset of XMM-Newton observations. We also applied the script to compute temporal properties of the sample of these spectra, namely, the energy resolved rms properties.

2 Sample

We selected a sample of public data in XMM archive that corresponds to pointed observations of AGNs – starting with 336 observations of 250 sources (selection from category *AGN, QSOs, BL-Lacs and XRB* made in spring 2004). Most of blazars where the disk emission would be damped in X-rays coming from the jet were rejected. Cross-correlation with Veron-Cetty catalogue (11th ed.) gave us redshift and AGN type for all but 24 targets. Out of these 226 AGNs, 84 have their counterparts in ROSAT Bright Source Catalogue. The average redshift was 0.72, however for those identified as Seyfert galaxies the value was 0.10 (the majority being S1-S1.5 with slightly higher redshift 0.13); AGN whose type was not identified in Veron had average redshift 2.21.

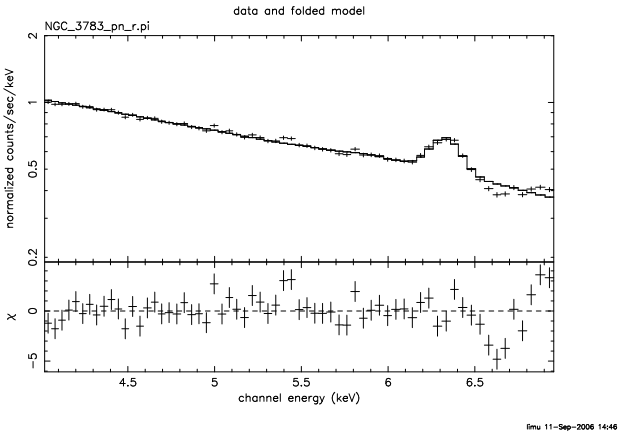

Fig. 1 Example of a spectrum fitted with power-law and two gaussian peaks (multiplied by warm absorber model), additional narrow lines can be searched in residuals shown below.

Since our main interest lies around the iron line, we use data only from PN and MOS cameras, in 1-10 keV range. The observations were taken mostly in Imaging regime, though the treatment of Timing mode was also included in the script.

3 Data processing

We start with raw data, applying standard pipeline (**emproc** and **epproc**) up to event-list level. Data of different subsets (window sizes) were combined using **merge** program of SAS, ending with a one file for PN and one for both MOS detectors. We leave out time intervals likely to be contaminated with cosmic rays, indicated by high count-rate ($>$ 10 ct/s) of photons above 10 keV. Then the 2-D image (in image coordinates with a pixel size corresponding to roughly 1 arcsec) is constructed and we look for a peak near the catalogue position of the source (mostly the boresight position). After that either event-list is reduced to events within 40 pixels of the barycentre of the peak. We also check for pile-up using **epatplot**.

Specific task is a generation of background data: from a collection of background exposures taken with different filters we cut-off a region corresponding to position of our target (after proceeding with **attcalc**). Background lightcurve is constructed from the actual dataset adjusting the hardness ratio to that of the pre-collected exposure.

Following the original purpose of the automated script, spectra were constructed using **evselect** and rebinned together with response matrices in a way that each spectral bin contains at least 25 events. Finally XSPEC (ver.11.3) was employed to fit the spectrum first in wide range (3$\sim$12 keV) using *pexrav* model, than in narrower band (4$\sim$7 keV) with an absorbed power-law continuum and several spectral lines of gaussian profile (starting with single line at the redshift-corrected iron line position).

4 Fine spectral analysis

Figure 1 shows as an example the spectrum of NGC 3783 obtained with PN detector in about 130 ksec – the average rate in the extracted region (before cuts in energy) was 12.5 ct/s. Besides the prominent iron line no significant second line is found. Since XSPEC often fails to localize weak and narrow lines, a proper routine was adopted that searches for most significant excesses (with sliding boxes of different sizes) in residual. However, so far no narrow line features were identified in the present dataset.

4.1 Separation of activity levels

Spectral variability is usually checked by comparison of states of higher and lower activity, measured with count rates in a specified energy band. The automated distinction of these states can be done from a histogram of rate values within given observation, however, this method works mostly only in the case of bimodal regime; for multiple states of more variable rates there is usually no clear separation in the histogram. The distinction can be done by identifying the state transitions with averaged absolute derivatives. Figure 2 shows part of the light-curve of MCG 6-30-15, that was smoothed afterwards with a convolution of a box of 1.5 ksec (to remove fast variability) and the absolute value of first differential was calculated – the green curve shows the sliding average – the most significant peaks correspond to transitions between different activity states. Different sizes of convolution (summing) windows were tested.

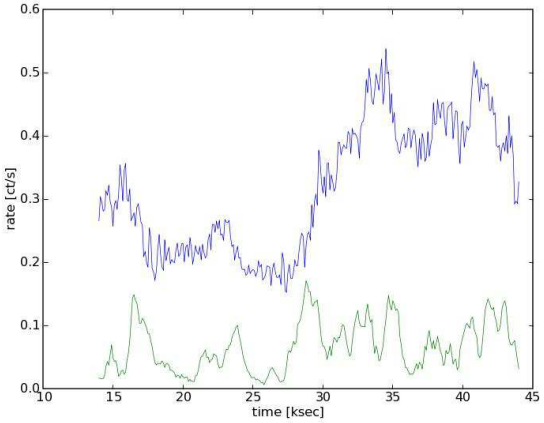

Fig. 2 Blue line shows PN rates (sliding averaged by 10 sec) from the extraction region of the source showing several levels of activity. Lower green line is the averaged absolute derivative.

The results are stored in a database that allows to check for many statistical properties – e.g. the Baldwin effect described in X-rays by Jiang et al. (2006). We also plan to extract more physical parameters (where statistics permits) from the shape of the Kα line using the latest XSPEC models, e.g. the *ky* model by Dovciak et al (2004).

5 Time-energy maps

One of the principal drawbacks of the previous approach is that fast spectral variations are lost in the average spectrum, so for example if the narrow line moves its center during the exposure time, it would be smeared out in the result. Having the selected event-list at hand, it is easy to construct a 2-D map with constant time bins in one direction and exponentially growing energy bins in the other. Number of bins being limited only by the statistics available, our initial choice is time sampling of 100 s and rather rough spectral resolution of 20 bins in 1$\sim$10 keV range. This allows us to sum-up data from PN and MOS detectors that is otherwise not possible with precise energy sampling.

The principle of such 2-D mapping was first described in detail in Iwasawa et al. (2004) for the case of NGC3516. Periodic iron line variations were detected between 5.5 and 6.5 keV in 2-ksec sampling; extensive simulations were used to derive the significance of observed excesses.

5.1 Normalization and GTI generation

To normalize properly the 2-D map (so that it can be displayed with the same scale in all energy bins), we have to

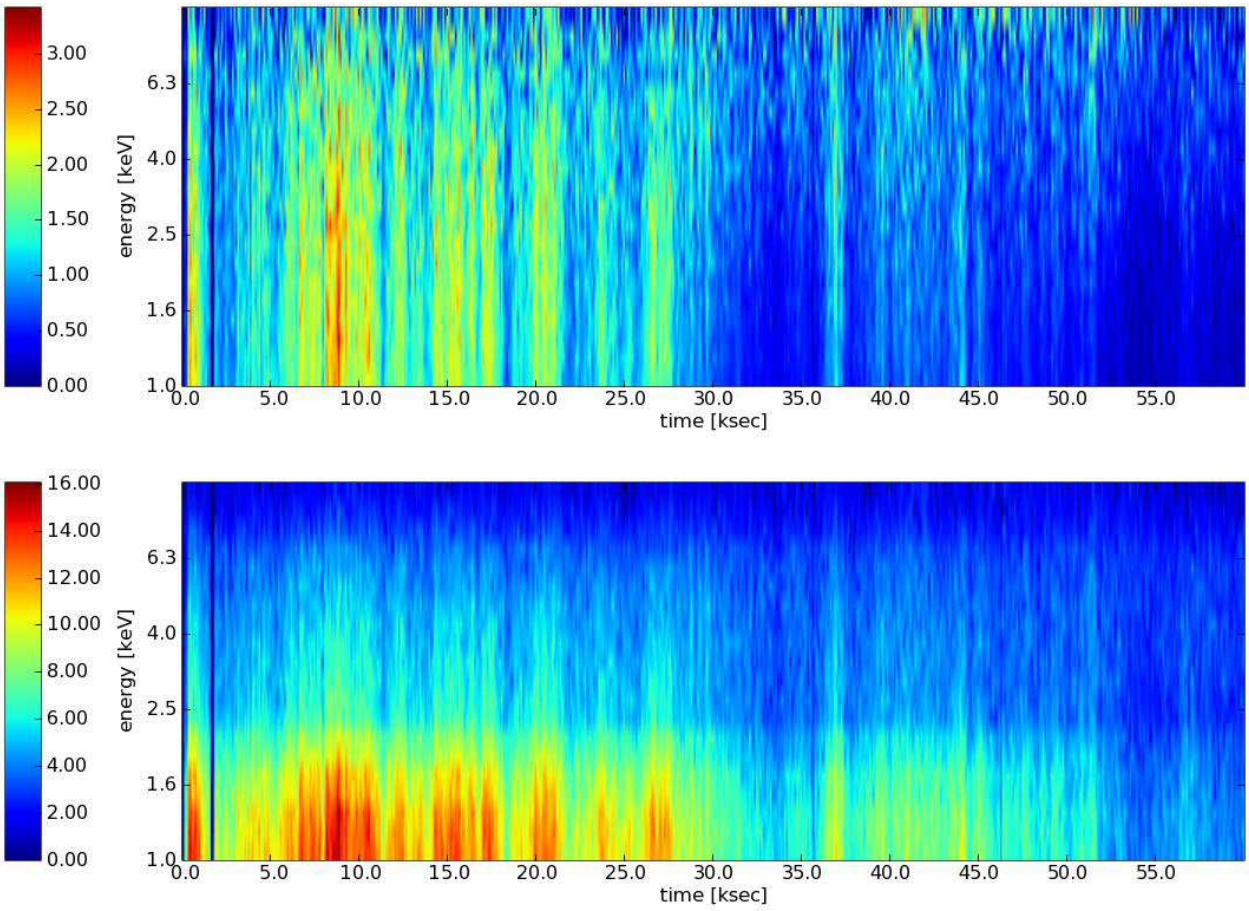

Fig. 3 Above: NGC 4051 normalized color-coded spectrum plotted in the time-energy domain. Below: the significance map of individual bins of the spectrum shown above; we notice that at higher energies (>6 keV) time binning should be coarser to confirm statistically significant results, which would clearly require to increase S/N of the data.

omit the periods of very low rate. This is done by setting the lower limit to the half of the value of bottom 20%. On the other hand, high count rate periods (measured at top of the spectrum, >10 keV) are also to be excluded from *good-time intervals* (GTI) because of probably large contamination with cosmic ray background. In each time bin the spectrum is then divided by average spectral shape, and 1 is subtracted, so the spectral and time variations cause the fluctuations around mean value 0. For the case of NGC 4051 (fig. 3) slight variations in the vicinity of iron line might be observed, too.

5.2 RMS variations

From these time-energy maps it is straightforward to construct the maps of variability over a longer time scale (say 1 ksec). This study was motivated by the fact that periods of increased fluctuation were observed during outburst with energy-dependent onset time (Ponti et al. 2004). We calculate the sliding sums and square sums using given windows (e.g. 11-bins) and get the map from the difference of these two. Figure 4 shows some typical "pattern", however, no regularities that could be interpreted as "lags" were found so far.

The significance of the map was estimated using 4th central momentum μ_4, from which we can calculate variance of the variance

$$\left\langle \mathrm{var}(s^2) \right\rangle = \frac{(N-1)^2}{N^3}\mu_4 - \frac{(N-1)(N-3)}{N^3}\mu_2^2 \qquad (1)$$

The significance value (ratio of the map shown and the square root of the corresponding value above) fluctuates considerably on a very short time scale, the average value for our example (quite flat over time) is about 7. The choice of the window size is done considering the length of different GTIs – obviously, they have to be treated separately.

5.3 Power spectrum

If the GTI interval is long enough a power spectral density distribution can be constructed in each energy band – at fig. 5 there are cases (MCG-6-30-15 and PKS 0558-504) that show some periodic signatures at low energies. We used a complex procedure for constructing PSD implemented in

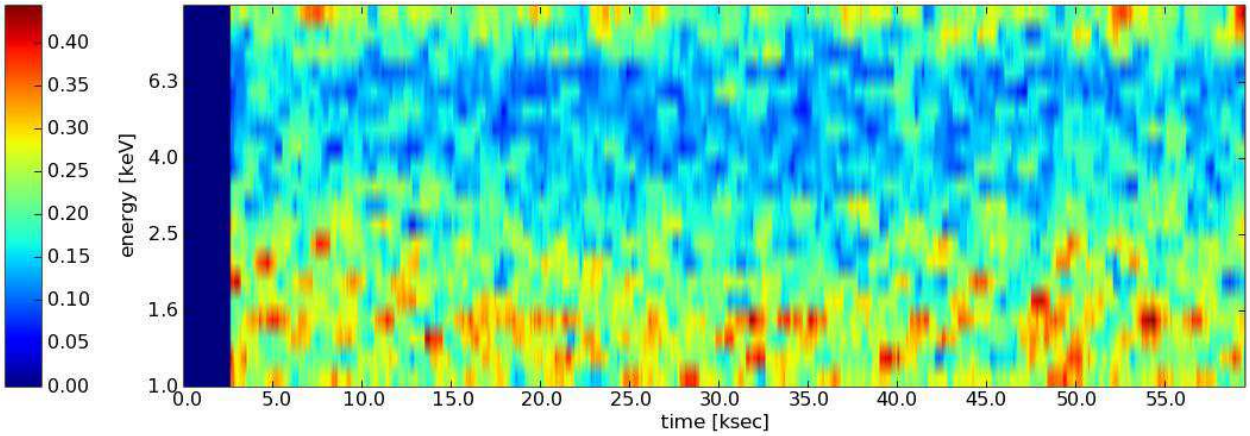

Fig. 4 Root mean square map of one observation of NGC 4151, using 11-bin variances. Also in this representation of the rms characteristics the plot indicates a widely discussed reduction of the source variability near the iron line energy.

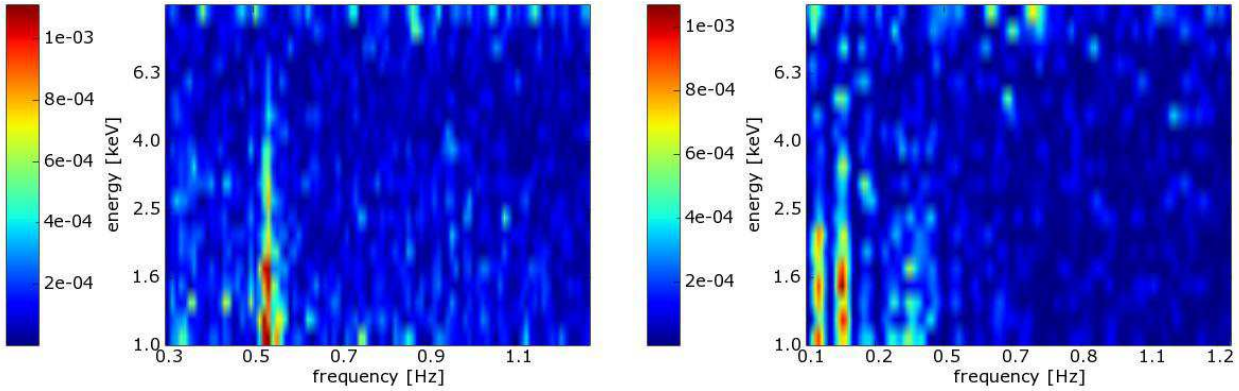

Fig. 5 Power spectral densities in 20 energy bands and 129 frequency bins. Color scale is logarithmic. The emerging features might (especially in the second case) have some instrumental origin.

pylab package of matplotlib (analysis and visualization routines for python, similar to MatLab) with capabilities to remove linear trends in individual segments. Wavelet analysis might be more fructiferous, as seen in recent results from Lachowicz et al (2006), however, it is not evident how to display the extra dimension. The time base we use is also considerably shorter than that suggested in this article – our further searches will extend the frequency range in this direction. For the moment we also don't have any estimation of the significance of any excesses – we plan to recourse for Monte-Carlo in this case.

6 Conclusions

The use of time-energy maps seems to be an interesting tool for discovery of variable, either periodic or non-periodic, spectral features in the emission of accretion disks. We used our analyzed sample of AGN data from PN and MOS detectors on XMM, and found a proper normalization to display it on the same scale in range of 1-8 keV. For the sake of statistics, we sacrificed the fine energy resolution of these instruments, dividing the spectrum in 20 bins only, while keeping the 100 s time bins. It allowed us to look also for changes in variability and construct the power spectrum density maps. As a discovery tool, it will need a thorough testing of any feature discovered with the help of fine spectral analysis, the original aim of our project. We present only some of the most interesting figures here, others can be found at **http://zeus.asu.cas.cz/xmm/res/maps/**.

References

Dovciak, M., Bianchi, S., Guainazzi, M. et al.: 2004, MNRAS 350, 745
Dovciak, M., Karas, V., Yaqoob, T.: 2004, ApJS 153, 205
Iwasawa, K. , Miniutti, G., Fabian, A.C.: 2004, MNRAS 355, 1073
Jiang, P. , Wang, J. X., Wang, T. G.: 2006, ApJ 644, 725
Lachowicz, P., Czerny, B. et al: astro-ph/0607594
Ponti, G., Cappi, M., Dadina, M. et al: 2004, A&A 417, 451
Turner, T.J., Kraemer, S.B., George, I.M., et al.: 2004, ApJ 618, 155
Yaqoob, T. , George, I.M., Kallman, T.R. :2003, ApJ 596, 85

